Analysis of Long Fibers Direction of Transversely Isotropic Hyperelastic Material for Thermoforming Application

F. ERCHIQUI*
Université du Québec en Abitibi-Témiscamingue, DSA
445 boulevard de l'Université, Rouyn-Noranda (Québec), J9X 5E4, Canada

A. BENDADA
Industrial Material Institute, CNRC, Boucherville, J4B 6Y4, Canada

A. GAKWAYA
Université Laval, 1314-F Pavillon Adrien-Pouliot
Sainte-Foy, Québec, Canada

ABSTRACT: In this work, we present the modeling and numerical simulation using the explicit dynamic finite element method for the hyperelastic behavior of a thin, transversely isotropic and incompressible thermoplastic membrane. The Lagrangian formulation together with the assumption of the membrane theory is used. The numerical validation is performed by comparing the theoretical solution for the uniaxial and equibiaxial Hencky deformation with the numerical results. Moreover, the effect of the transversely hyperelastic material on the thickness and on the stress distribution, for the membrane inflation, are analyzed for three different fibers orientations. Finally, a simple example of thermoforming part is presented.

KEY WORDS: long fibers, viscoelasticity, finite element, thermoforming.

INTRODUCTION

SEVERAL PRACTICAL APPLICATIONS in engineering are related to the thermoplastic materials reinforced by continuous fibers. By way of example, one can quote the sector of the material-forming processes (thermoforming processes) for man-made composites for the automobile and the aerospace applications and the sector of biomechanics for the biological composites for soft biological tissues such as blood vessels, tendons, and ligaments. However, the response of these materials to loads, either in pressure or flow, depends on the mechanical and rheological properties of the polymeric matrix, the fibers, and the fiber–polymeric matrix interactions. From this point of view, the structural properties of such composites may be regarded as anisotropic as opposed to isotropic materials, which exhibit no directional dependencies.

*Author to whom correspondence should be addressed. E-mail: fouad.erchiqui@uqat.ca

0731-6844/05/09 0961–15 $10.00/0 DOI: 10.1177/0731684405048196

In the past decades, it has been noticed that many research tasks have been directed toward the use of the behavior law of the hyperelastic and viscoelastic isotropic type, for the processes of thermoforming of thin parts. In the case of hyperelastic materials, the constitutive laws of Mooney-Rivlin [21] and Ogden [20] are used to describe, in general, the structural behavior of the investigated membranes [1,7,10,17,22]. In the case of viscoelastic membranes, their constitutive behavior uses the integral models of Lodge [19], Christensen [5] and very recently the models of K-BKZ [23] were considered to be the most suitable to describe the polymeric membrane behavior [10,13,14,17,24] . For these models, the finite element implementation of large strain isotropic materials are well established and most successfully used in industrial processes, and particularly for the thermoforming and blowing processes.

However, the studies concerning the construction of theories and numerical models to describe the structural behavior of the anisotropic thermoplastic membranes (membranes reinforced by continuous fibers) are very recent and the publications which are devoted to them are quite a few. The papers by [2,3,4,15,25], describe constitutive equations for fiber-oriented hyperelastic materials in the nonlinear stress and deformation domain and provide computational informations for their finite element implementation. Also, works dealing with the influence of the fibers orientation on the behavior of the hyperelastic membranes and the applications which come under the field of thermoforming remain relatively scarce.

The goal of the present paper is thus the study of the influence of the fiber orientation on the behavior of the transversely isotropic hyperelastic membranes for thermoforming applications. The strain energy which takes into account the anisotropy induced by the presence of fibers aligned in the membrane is considered [2,18,25,26]. Mathematical modeling and numerical simulation using the explicit finite element method are considered for the study of hyperelastic behavior of a thin, transversely isotropic and incompressible thermoplastic membrane. The thermoforming of the long fiber-reinforced sheet is done under the action of a perfect gas [12]. The Lagrangian formulation together with the assumption of the membrane theory is used. The membrane is discretized by plane finite element [8] and time integration is performed via an explicit algorithm [9].

The numerical analysis is performed by comparing the obtained results with the analytical results for the uniaxial and equibiaxial Henky deformation (with or without fibers). Moreover, the influence of the orientation of the fibers on the thickness and the stress distribution in the thermoforming sheet is analyzed.

PRELIMINARY CONSIDERATIONS

The problem of the transversely isotropic thermoplastic sheet material inflation can be modeled by considering the large deformation of the body with finite strain. The continuum formulation using the updated Lagrangian description is presented using a three nodes isoparametric triangular element. Although the formulation is applicable for three-dimensional geometry, the finite element discretization is shown for plane strain configuration only, for the sake of simplicity.

FINITE ELEMENTS FORMULATION

For the numerical modeling of thermoplastic membrane inflation, we consider the explicit dynamic finite element method, based on the Lagrangian formulation, with both

space and time discretization to perform the simulation of the membrane inflation. In the spatial discretization, we subdivide the material sheet into isoparametric triangular finite elements using three nodes. Then the principle of virtual work is written on each of these elements with a local finite element approximation and evaluated to yield discrete element equations which are then assembled so as to form an approximate membrane representation [8]. Under these conditions, the problem of thermoplastic sheet material inflation can then be reduced to a system of second-order ordinary differential equations [11]:

$$[M] \cdot \{\ddot{u}(t)\} = \{F_{\text{ext.}}\} - \{F_{\text{int.}}\} \tag{1}$$

where $\{F_{\text{ext.}}\}$ and $\{F_{\text{int.}}\}$ are global nodal external and internal force vectors experienced by the thermoplastic membrane. $[M]$ is the mass matrix associated with external forces.

Using the diagonalization method of [16], matrix $[M]$ is transformed into a diagonal matrix and each degree of freedom can then be handled independently.

Because of the presence of the inertial force, a time discretization is required. This is handled here through the introduction of a centerd finite difference technique that is conditionally stable [9].

The convergence behavior of the explicit dynamic finite element method for nonlinear problem is controlled by the Courant–Friedrichs–Lewy criterion: the time step must be smaller than the critical time steps Δt_{crit}:

$$\Delta t \leq \Delta t_{\text{crit}} \sim h/c \tag{2}$$

Here c is the wave speed in the medium and h, the element size. The quantity h/c is the time that a wave needs to propagate across an element of size h.

PRESSURE LOADING

In this work, we consider the outside pressure forces induced by the load and the airflow responsible for the blowing of the membrane. The pressure inside the thermoplastic membrane is closely related to the internal volume of the parison via the perfect gas thermodynamic law by [12]:

$$\Delta P(t) = P(t) - P_0 = \frac{n(t)RT_{\text{gas}} - P_0 V(t)}{V_0 + V(t)} \tag{3}$$

V_0 is the initial volume enclosing the membrane at the initial time t_0 (we assume in this work that the forming process temperature is constant, T_{gas}), P_0 is the initial pressure, R is the perfect gas constant, $n(t)$ is the number of gas moles, introduced for the inflation of the thermoplastic membrane, $P(t)$ is the internal pressure and $V(t)$ is the volume occupied by the membrane at time t.

TRANSVERSELY ISOTROPIC HYPERELASTICITY MATERIAL

In this work, we consider the assumptions of the plane stresses and the incompressibility of the thermoplastic material. It follows that the components of the Cauchy stress tensor have the following properties:

$$\sigma_{13} = \sigma_{23} = \sigma_{31} = \sigma_{32} = \sigma_{33} = 0 \tag{4}$$

The transversely isotropic hyperelastic materials are defined by the existence of the strain energy density function, W, from which stresses can be derived at each point. By choosing the following form for strain energy density function for transversely isotropic hyperelastic materials [2,25]:

$$W = W(\vec{X}, I_1(\mathbf{C}), I_2(\mathbf{C}), I_3(\mathbf{C}), I_4(\mathbf{C}, \vec{A}), I_5(\mathbf{C}, \vec{A})) \tag{5}$$

the satisfaction of material frame indifference and the material symmetry restrictions imposed by the orientation of fibers in the thermoplastic materials are assured (principal of objectivity). I_1, I_2, and I_3 are the isotropic standard invariants of the right Cauchy–Green deformation tensor, $\mathbf{C}$. I_4 and I_5 are the pseudoinvariants introduced by the fiber family in thermoplastic material. These pseudoinvariants represent contributions to the strain energy function from the properties of the fibers and their interaction with the thermoplastic matrix. The vector $\vec{A}$ is a material director of aligned fibers in material configuration. The expressions of these invariants are given by the following formulas:

$$I_1 = tr\,\mathbf{C}; \quad I_2 = \mathbf{C} : \mathbf{C}; \quad I_3 = \det \mathbf{C} = J^2; \quad I_4 = \vec{A} \cdot \mathbf{C} \cdot \vec{A}; \quad I_5 = \vec{A} \cdot \mathbf{C}^2 \cdot \vec{A} \tag{6}$$

where J is the Jacobian of deformation. The general stress–strain relationship is given by the formula:

$$\mathbf{S} = 2\frac{\partial W}{\partial \mathbf{C}} \tag{7}$$

where $\mathbf{S}$ is the Piola–Kirchhoff stress tensor. Differentiating the expressions (6) with respect to $\mathbf{C}$ gives:

$$\frac{\partial I_1}{\partial \mathbf{C}} = \mathbf{I}; \quad \frac{\partial I_2}{\partial \mathbf{C}} = I_1\mathbf{I} - \mathbf{C}; \quad \frac{\partial I_3}{\partial \mathbf{C}} = I_3\mathbf{C}^{-1}; \quad \frac{\partial I_4}{\partial \mathbf{C}} = \vec{A} \otimes \vec{A}; \quad \frac{\partial I_5}{\partial \mathbf{C}} = \vec{A} \otimes \mathbf{C}\vec{A} + \mathbf{C}\vec{A} \otimes \vec{A} \tag{8}$$

where $\mathbf{I}$ is the identity tensor. The second Piola–Kirchhoff stress tensor, given by Equation (7), becomes:

$$\mathbf{S} = 2\psi_1\mathbf{I} + 2\psi_2(I_1\mathbf{I} - \mathbf{C}) + 2I_3\psi_3\mathbf{C}^{-1} + 2\psi_4\vec{A} \otimes \vec{A} + 2\psi_5\left(\mathbf{C}\vec{A} \otimes \vec{A} + \vec{A} \otimes \mathbf{C}\vec{A}\right) \tag{9}$$

The scalar ψ_i denotes the derivation of W with respect to I_i:

$$\psi_i = \frac{\partial W}{\partial I_i}; \quad i = 1, 2, 3, 4, 5 \tag{10}$$

Within the framework of the incompressible material, $I_3 = J^2 = 1$, the strain energy function can then be written as:

$$W = \Psi_1(I_1, I_2) + \Psi_2(I_4) + \Psi_3(I_1, I_2, I_4, I_5) \tag{11}$$

The function Ψ_1 represents the material response of the isotropic thermoplastic sheet, Ψ_2 the contribution response from the fiber family in the thermoplastic material and Ψ_3 the

contribution response from interactions between the fibers and the thermoplastic matrix. In this case, the general incompressible transversely isotropic hyperelastic constitutive equation can be calculated by the formula:

$$\mathbf{S} = -p\mathbf{C}^{-1} + 2\frac{\partial W}{\partial \mathbf{C}} \tag{12}$$

where p is the hydrostatic pressure. This pressure, which enters Piola–Kirchhoff stress tensor as a reaction to kinematic constraint on the deformation field, is determined by using Equation (9) and the condition $S_{zz} = 0$:

$$p = 2\left(\frac{2\Psi_1 + \Psi_2\left(C_{xx} + C_{yy}\right)}{C_{xx}C_{yy} - C_{xy}C_{yx}}\right) \tag{13}$$

By considering formula (13), the expression of the second Piola–Kirchhoff stress tensor, Equation (23), then becomes:

$$\mathbf{S} = -p\mathbf{C}^{-1} + 2\psi_1\mathbf{I} + 2\psi_2(I_1\mathbf{I} - \mathbf{C}) + 2\psi_4\vec{A}\otimes\vec{A} + 2\psi_5\left(\mathbf{C}\vec{A}\otimes\vec{A} + \vec{A}\otimes\mathbf{C}\vec{A}\right) \tag{14}$$

In our study, for the plane stress state, the deformation matrix $\mathbf{C}$, the stress matrix $\mathbf{S}$, the fiber matrix orientation $\mathbf{A}(=\vec{A}\otimes\vec{A})$ and the interaction matix $\mathbf{M}(=\mathbf{C}\vec{A}\otimes\vec{A} + \vec{A}\otimes\vec{A}\mathbf{C})$, between the fibers and the thermoplastic material, have respectively the following forms:

$$[\mathbf{C}] = \begin{bmatrix} C_{xx} & C_{xy} & 0 \\ C_{xy} & C_{yy} & 0 \\ 0 & 0 & C_{zz} \end{bmatrix} \tag{15}$$

$$[\mathbf{S}] = \begin{bmatrix} S_{xx} & S_{xy} & 0 \\ S_{xy} & S_{yy} & 0 \\ 0 & 0 & 0 \end{bmatrix} \tag{16}$$

$$\mathbf{A} = \vec{A}\otimes\vec{A} = \begin{bmatrix} A_1A_1 & A_1A_2 & 0 \\ A_1A_2 & A_2A_2 & 0 \\ 0 & 0 & 0 \end{bmatrix} \tag{17}$$

$$\mathbf{M} = \begin{bmatrix} 2\left(C_{xx}A_1^2 + C_{xy}A_1A_2\right) & A_1A_2\left(C_{xx} + C_{yy}\right) + C_{xy}\left(A_1^2 + A_2^2\right) & 0 \\ \text{Symmetric} & 2\left(C_{yy}A_2^2 + C_{xy}A_1A_2\right) & 0 \\ 0 & 0 & 0 \end{bmatrix} \tag{18}$$

The term C_{zz} in Equation (15) can be directly computed from the other components of the deformation tensor:

$$C_{zz} = \lambda_3^2 = \frac{1}{C_{xx}C_{yy} - C_{xy}C_{xy}} \tag{19}$$

where λ_3 is the principal stretch ratio in the thickness direction defined by:

$$\lambda_3 = \frac{h}{h_0} \tag{20}$$

where h and h_0 are membrane thicknesses, respectively in the deformed and undeformed configurations.

For the adopted strategy for the computer implementation of the finite element formulation, developed above for the computation of the nodal displacements $\vec{u}_n$ at a time t_{n+1}, see [11].

NUMERICAL VALIDATION

The dynamic finite element method outlined in the previous section was implemented in the general purpose finite element code ThermoForm, developed by the first author. The transversely isotropic hyperelastic material described earlier has been used. This code was developed in order to study the stresses and deformation arising in thermoforming sheet problems. A simple example of the use of the transversely isotropic material in this code is presented here. All computations were performed on PC in single precision.

Validation of Piola–Kirchhoff Stress

As a validation of the formulation described earlier, we consider the uniaxial and equibiaxial tests. For these tests, we consider a Mooney-Rivlin thermoplastic material for $\Psi_1(I_1, I_2)$ and a linear function for $\Psi_2(I_1, I_2)$:

$$\Psi_1(I_1, I_2) = C_1(I_1 - 3) + C_2(I_2 - 3); \quad \Psi_2(I_4) = C_4(I_4 - 1) \tag{21}$$

C_1, C_2, and C_4 are the material constants.

The stress update was validated by comparing the results from uniaxial and equibiaxial tests with a theoretical solution for a homogeneous Hencky deformation:

$$\lambda(t) = \exp(at) \tag{22}$$

where $\lambda(t)$ is the stretch deformation and a is the rate of deformation. The material constants used for these tests are:

$$C_1 = 1{,}000{,}000\ Pa, \quad C_2 = 1000\ Pa, \quad C_4 = 100{,}000 \tag{23}$$

For the uniaxial Hencky deformation, the initial membrane configuration is a rectangular sheet (length = 10 units, width = 1 unit), while for the equibiaxial Hencky deformation, the initial membrane configuration is a square sheet (width = 1 unit). The thickness considered in these tests is $h = 0.1$ unit. A mesh of triangular elements was used comprising five nodes and four elements. The meshes used for the uniaxial (Mesh 1) and the equibiaxial (Mesh 2) test are represented in Figure 1. The timestep is controlled by a stability criterion (Courant–Friedrichs–Lewy criterion) where the distance traveled by the viscoelastic waves over a single timestep is not greater than 75% of the smallest element

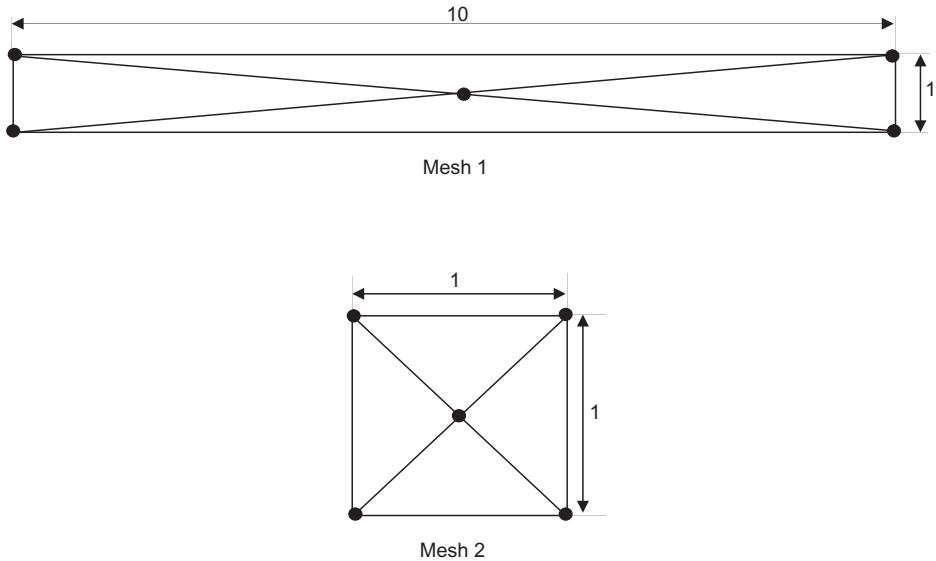

Figure 1. *Finite element meshes : Mesh 1 for uniaxial test and Mesh 2 for equibiaxial test.*

size. For the isotropic case (without fibers), Figures 2 and 3 illustrate the excellent agreement between the theoretical and the dynamic finite element solutions for three different fiber directions.

For the uniaxial and equibiaxial problems, the elements were stretched to 500% of their initial length for a deadline of 0.2 s and with equal timesteps of 0.0001 s.

ANALYSIS OF FIBERS DIRECTION EFFECT DURING FREE MEMBRANE BLOWING

In this section, we use the dynamic finite element approach, with a linear air flow load, to study the effect of long fibers direction the thickness and the stress distribution in the rectangular thermoplastic sheet during its free blowing. The time of blowing in this study is fixed at 0.5 s. The geometry of the undeformed sheet configuration used in the simulation is $L = 25.4$ cm (length), $l = 15.24$ cm (wide) and $h_0 = 1.5$ mm (thickness). The sheet is discretized by triangular membrane elements and its sides are fixed. Mechanical parameters used for this study are given earlier. In Figure 4, we present the evolutions of the deformations $(\lambda_1, \lambda_2, \lambda_3)$ in the case of free blowing of the rectangular membrane (without fibers).

Figures 5 and 6 present, respectively, the effect of the fibers direction on the minimal thickness distribution and the maximal von Mises stresses, σ_{eq}, distribution, induced by the blowing pressure on the thermoplastic sheet at the end of the blowing cycle ($t = 0.5$ s). From these figures, we observe that the thicknesses distribution reaches a minimal value, $h = 0.0408$ mm, and the von Mises stresses distribution passes by a maximal value, 7.22 MPa. These critical values are obtained for the direction $\theta = 55^\circ$, of fibers in the thermoplastic sheet. These values are localized with the approximate position: $X \simeq 2L/3$ and $Y \simeq l/2$ of the reference configuration. The highest value of the minimal thickness distribution, $h = 0.0507$ mm, and the minimal value of the von Mises stresses distribution are obtained for $\theta = 0^\circ$.

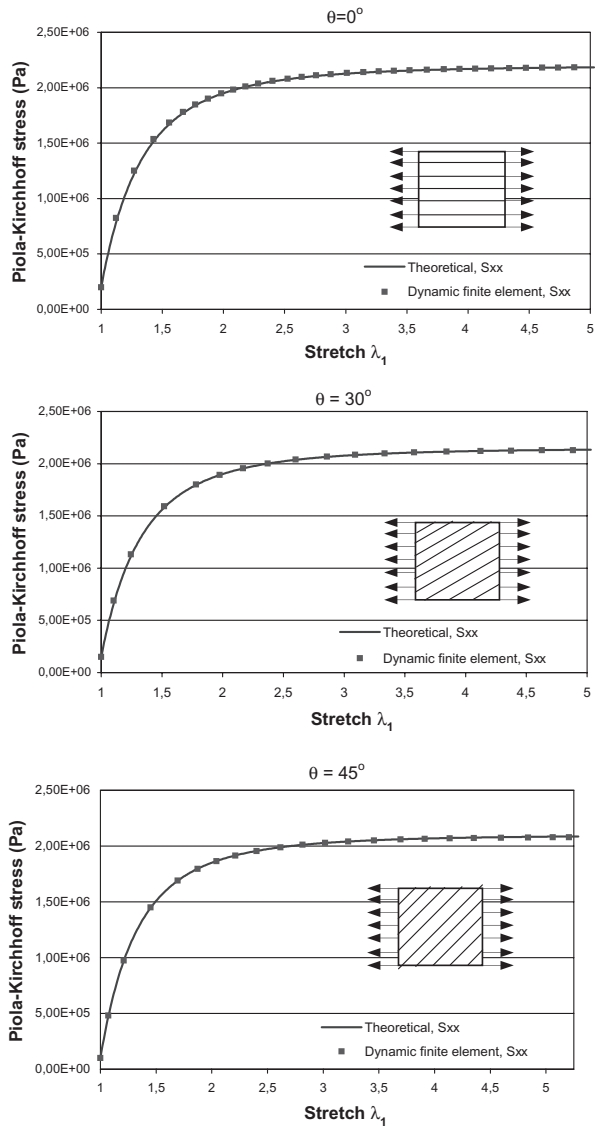

Figure 2. *Comparison of DFEM results to theoretical answer for uniaxial extension.*

According to these observations, one can thus conclude that in free blowing from a rectangular thermoplastic sheet reinforced with continuous long fibers, for a given time of blowing and airflow, there seems to exist a relationship between the orientation of the fibers and the stresses distribution which are developed in the material. This critical stress function passes by a maximum for a critical value of orientation, in our case this value is $\theta = 55^{\circ}$. In addition, to this critical value, there corresponds a critical minimal thickness. Indeed, the localized thinning effect of the deformed membrane is generally accompanied by an increase in the Cauchy stresses or the true stresses of the material.

In consequence of these remarks, for a given airflow load , the stresses induced in a part must depend on the initial orientation of the continuous fibers in the thermoplastic sheet.

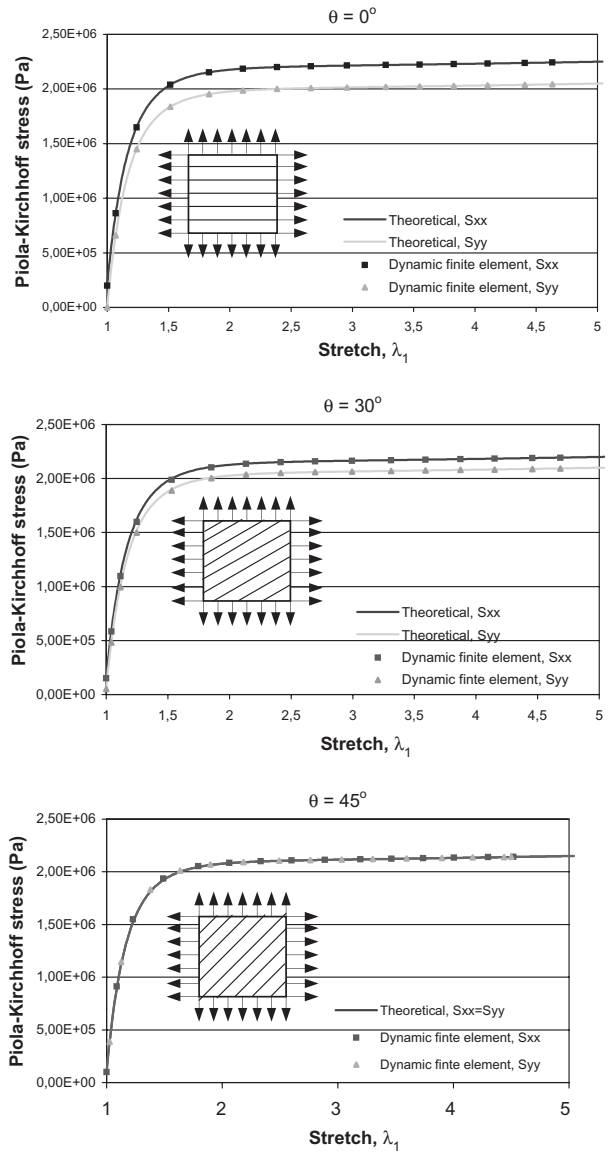

Figure 3. *Comparison of DFEM results to theoretical answer for equibiaxial extension.*

The above example is devoted for a simple thermoforming of a container with three different orientations of fibers.

EXAMPLE OF THERMOFORMING APPLICATION

In this section, we use the linear airflow, to study the thermoforming of a polymeric container. The geometries of mold, with a grid using the triangular membrane elements, is presented on Figure 7. We consider the same thermoplastic sheet as that used in the previous section, as well as the mechanical parameters.

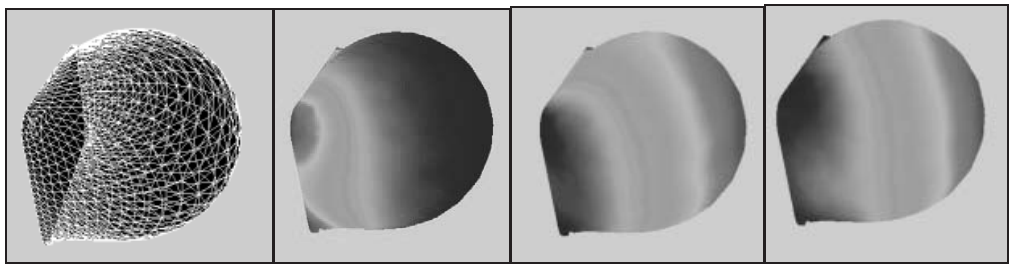

Figure 4. *Evolution of the deformations in the case of free blowing of the membrane.*

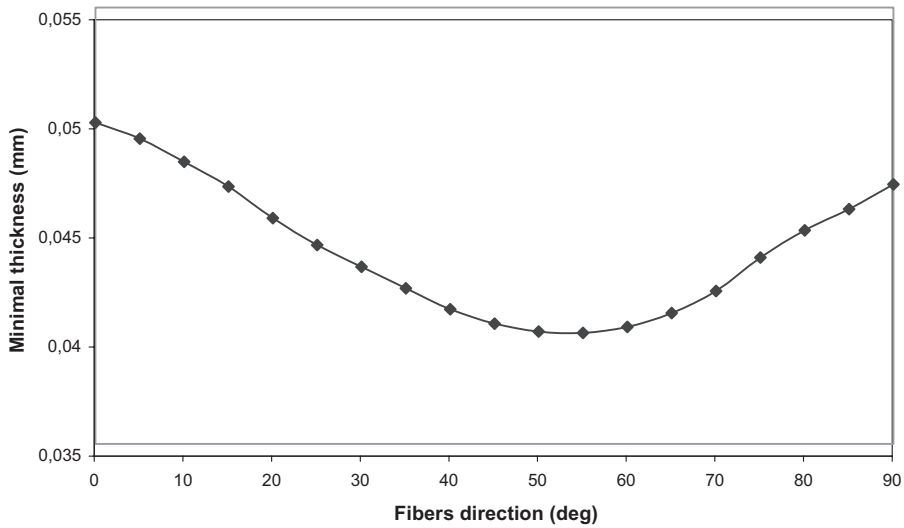

Figure 5. *Effect of the orientation of fibers on the distribution critical thicknesses.*

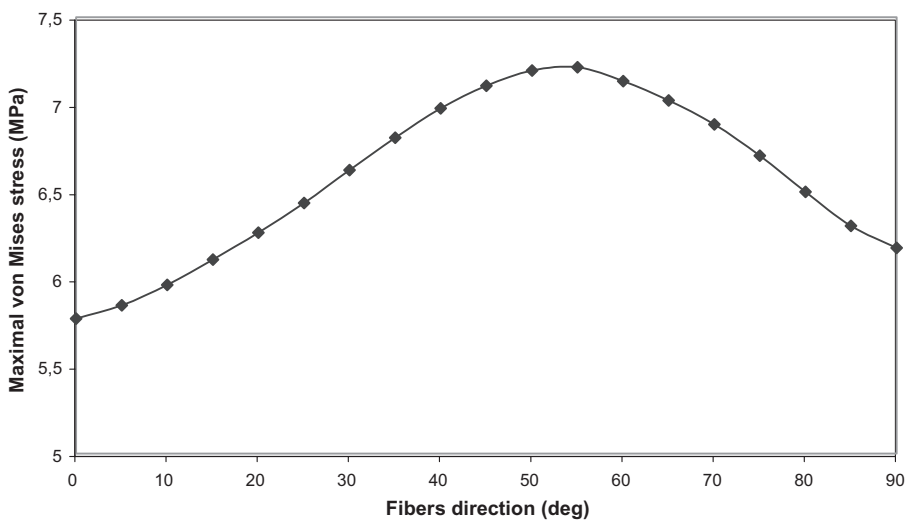

Figure 6. *Effect of the orientation of fibers on the distribution critical von Mises stress.*

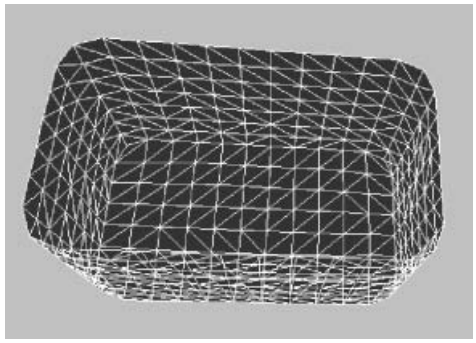

Figure 7. *Finite element meshes for mold.*

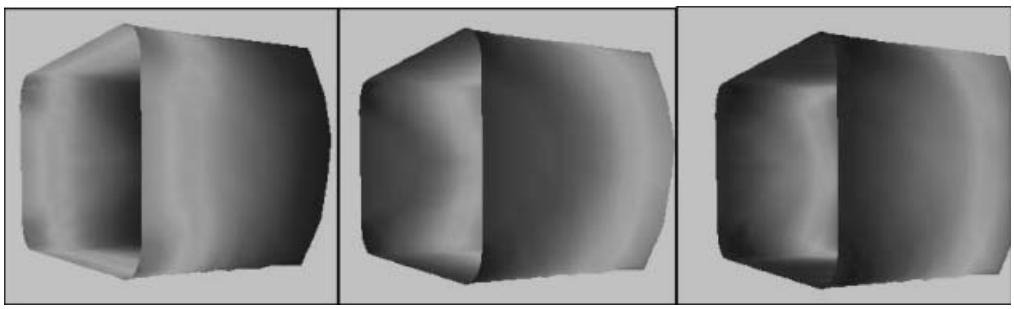

Figure 8. *Distribution of the deformations in the thermoformed container.*

The directions considered, in this work, for the fibers orientation in the materials are: $\theta = 0$, 30, and 45°. For the contact of the preform and the mold, we consider the assumption of sticking contact, because it is estimated that the polymer cools and stiffens quickly and that the pressure of working is not sufficient to deform the part of the parison which is in contact with the mold [6].

Figure 8 presents different deformation views ($\lambda_1, \lambda_2, \lambda_3$), at the end of the thermoforming process, induced in the final shape for $\theta = 0°$.

Figure 9 presents, the final thickness distribution $h = h_0\lambda_3$ on the half-planes of symmetry XZ and YZ in the thermoformed container for the three directions of fibers. From these figures, we observe a maximum thinning of 10.4%, reached with the respective positions of 8.01 and 18.07 cm, while in the center of the lower part of the container, thinning is of 32.5%.

The comparison of the numerical results obtained, for the thermoforming of the thermoplastic part, shows that there is a small difference in the results predicted by our calculations of modeling for the three fibers direction in the material. However, one notices a shift in the distribution thicknesses. Indeed, in the vicinities of the edges of the part, thinning seems to decrease with the orientation of fibers, in the symmetry plane half XZ. On the other hand, in the medium of the central part, thinning seems to decrease with the orientation of fibers. This phenomenon is less predictive, in the half-plane YZ, in the case of the distribution of the stresses of von Mises. Indeed, the stresses of von Mises are low in the areas of edges for $\theta = 0°$ and high in the vicinities of the critical zone (X = 7.5 cm, y = 6.0 cm) for $\theta = 20°$. In the central part, the von Mises stresses are low for $\theta = 50°$ and high for $\theta = 0°$.

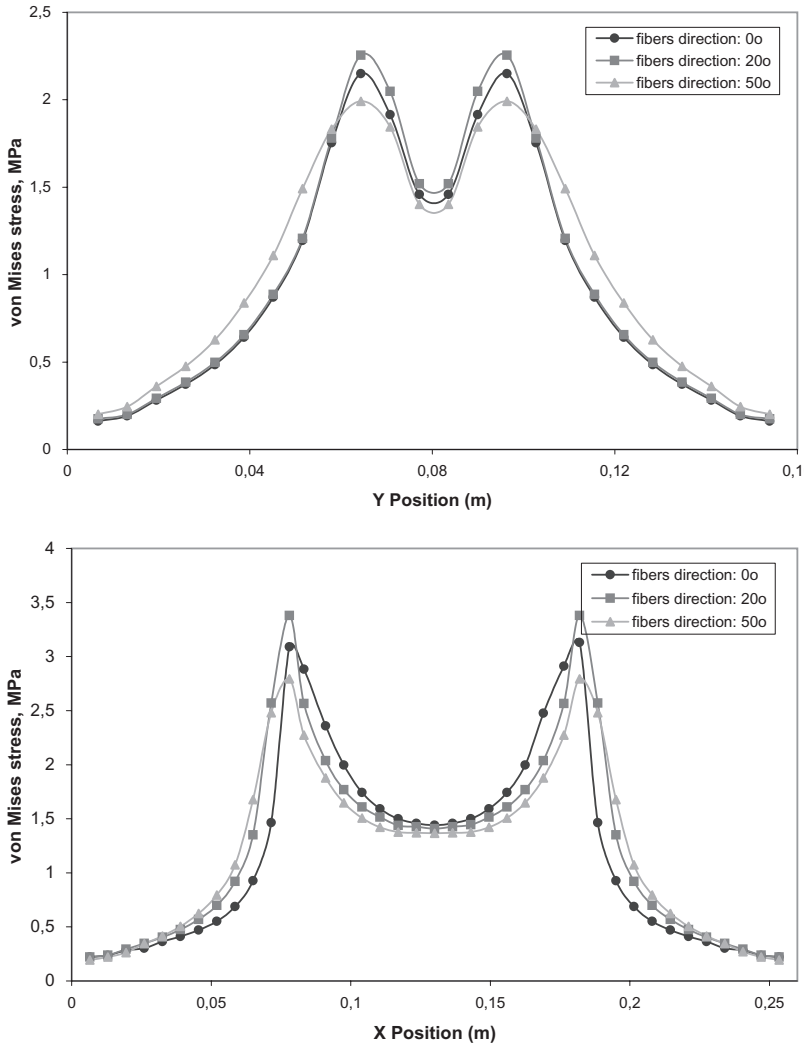

Figure 9. *von Mises stress distribution, symmetry planes XZ and YZ.*

In the thermoforming numerical simulation, the thickness prediction is an important goal but the stress estimation is also helpful for part design. Indeed, the prediction of the residual stress and the shape stability of the part are strongly related to the estimated stress. In this section, the stress prediction obtained from the investigated constitutive model for the three directions of fibers are discussed. Figure 10 presents the final von Mises stresses σ_{eq} distribution, predicted by using different fibers orientations, on the half-planes of XZ and YZ symmetry planes in the thermoformed container. The von Mises stress σ_{eq} on the half-plane XZ exhibit the maximum at the edges of the part and the minimum at the center of the part. A comparative study of the numerical results, obtained from the different fibers orientations, shows that there is a significant difference between the orientation $\theta = 20^{\circ}$ and the other orientation of fibers in the hyperelastic material, for the von Mises stress. In the half-plane XZ, the maximum value is obtained for $\theta = 20^{\circ}$ and the minimal value is obtained for $\theta = 50^{\circ}$. Finally, the von Mises stress distribution

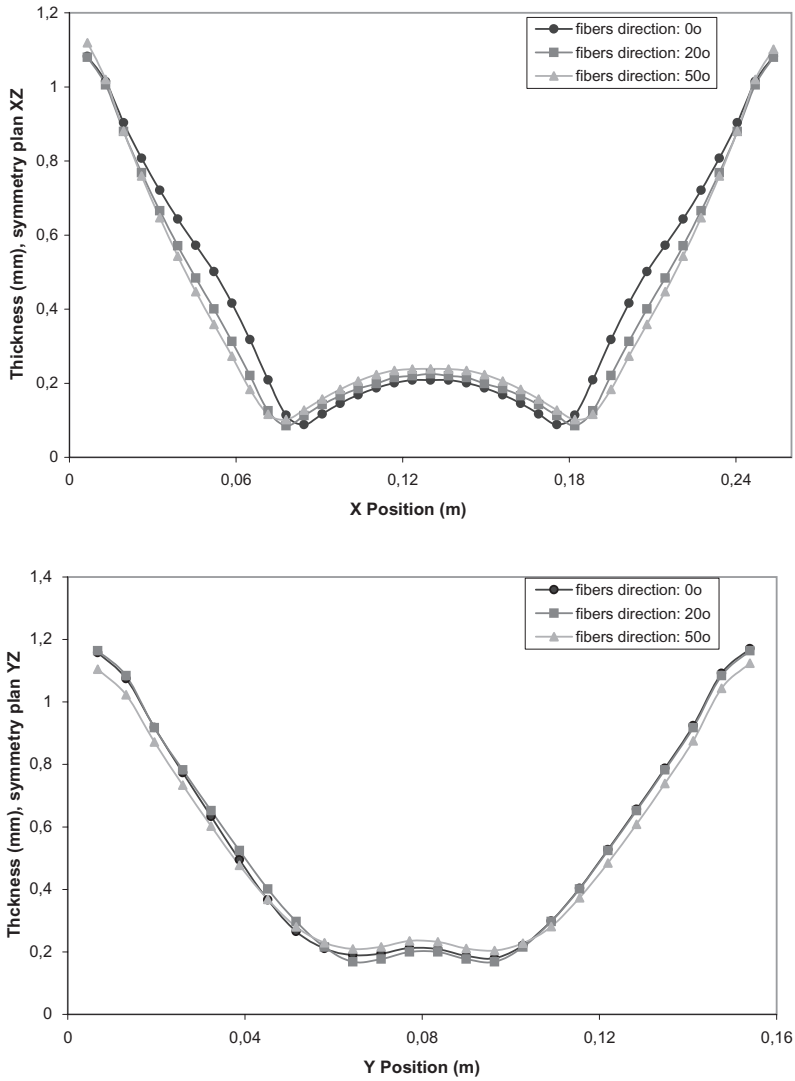

Figure 10. *Thickness distribution, symmetry planes XZ and YZ.*

plus the localized thinning effect indicate that material failure due to large deformation induced by inflation is most likely to occur at the edges of the container.

In the light of the results given earlier, the following remarks can be formulated:

- While the thickness distributions obtained from the different fibers directions of the transversely isotropic hyperelastic material are similar, the stress prediction exhibits some discrepancy. The similarity of the thickness distributions is related to the incompressibility assumption. This observation, concerning the isotropic and incompressible material thermoforming of hyperelastic type, was underlined by Lorenzi and Nied [6] relative with the final distribution thickness in the part. More recently, Erchiqui et al. noticed the same conclusion for viscoelastic materials [12]. According to these authors, this distribution thickness is not very dependent on the law of behavior

of material, but especially imposed by the geometry of the mold. Our study, concerning transversely isotropic hyperelastic material, also shows that the fibers directions influence very little the final distribution thickness of the thermoforming parts.

- The significant difference between the orientation of fibers for the transversely isotropic hyperelastic model is observed in the stress distribution at the end of the deformation. The maximum value is obtained for $\theta = 20^{\circ}$.

CONCLUSIONS

In this work, we have developed a dynamic finite element code based on the total Lagrangian formulation for simulating the response of the transversely isotropic hyperelastic material. The numerical analysis is performed by comparing the obtained results with the analytical results for the uniaxial and equibiaxial Henky deformation (with or without fibers). Then, we studied, in free blowing of a rectangular sheet, the effect of the orientation of fibers on the distribution thicknesses and stresses. The results obtained showed that these distributions pass by extremums. finally, we have studied the influence of three fibers direction in the transversely isotropic hyperelastic material on the thickness distribution in a hollow part, via air flow loading distribution. According to these results, one notices that the fibers directions influence a little the final distributions thickness and the von Mises stress of the thermoforming part.

These preliminary studies are essential steps toward the full achievement of our midterm goals of performing and developing tools for modeling and simulation of thermoplastic forming processes, as related in particular to the thermoforming processes.

ACKNOWLEDGMENTS

We fully acknowledge the NSERC for its financial support of this project on modeling and characterization of thermo-plastic polymers.

REFERENCES

1. Bonnet, J. and Burton, A. J. (2000). Finite Element Analysis of Air Supported Membrane Structures, *Computer Methods in Applied Mechanics and Engineering*, **190**: 579–595.
2. Bonnet, J. and Burton, A. J. (1998). A Simple Orthotropic, Transversely Isotropic Hyperelastic Constitutive Equation for Large Strain Computations, *Computer in Applied Mechanics and Engineering*, **162**: 151–164.
3. Bhattacharyya, D., Burt, C. R. and Martin, T. A. (1993). Forming of Fiber Reinforced Thermoplastic Sheets, In: *Advanced composites'93, International Conference on Advanced Composite Materials*, pp. 875–882.
4. Chevaugeon, N., Verron, E. and Peseux, P. (2000.). Finite Element Analysis of Nolinear Transversely Isotropic Membranes for Thermoforming Applications, In: *European Congress on Computational Methods in Applied Sciences and Engineering*, 11–14 September, Barcelona.
5. Christensen, R. M. and Carley, J. F. (1980). A Nonlinear Theory of Viscoelasticity for Application to Elastomers, *J. Appl. Mech. ASME*, **47**: 762–768.
6. DeLorenzi, H. G. and Nied, H. F. (1991). Finite Element Simulation of Thermoforming and Blow Molding, In: *Progress in Polymer Processing*, Vol. 1 – Modeling of Polymer Processing, pp. 117–171, Hanser Verlag.
7. DeLorenzi, H. G. and Nied, H. F. (1987). Blow Molding and Thermoforming of Plastics: Finite Element Modeling, *Compt. Structure*, **6**: 197–206.
8. Dhatt, G. and Touzot, G. (1984). *Une présentation de la méthode des éléments finis*, Collection Université de Compiègne, 2 ième édition.
9. Dokainish, M. A. and Subbaraj, K. (1989). A Survey of Direct Time-integration Methods in Computational Structural Dynamics, *Comput. Struct.*, **32**(6): 1371–1386.

10. Erchiqui, F., Derdouri, A., Gakwaya, A. and Verron, E. (2001). Analyse expérimentale et numérique en soufflage libre d'une membrane thermoplastique, *Entropie*, **235/236**: 118–125.
11. Erchiqui, F. and Gakwaya, A. (2003). Modélisation du comportement viscoélastique d'une membrane thermoplastique par la méthode des éléments finis, *Revue européenne des éléments finis*, **12**(1): 43–58.
12. Erchiqui, F. and Gakwaya, A. (2003). Analysis of Gas Pressure Effect during the Thermoplastic Membrane Forming using the Dynamic Finite Element Method, In: *PPS-19, Annual Polymer Processing Society, Session 7 : Blow Moulding and Thermoforming*, 7–10 July, Melbourne, Australia.
13. Erchiqui, F., Gakwaya, A. and Rachik, M. (2003). Analysis of Gas Pressure Effect during the KBK-Z Polymer Membrane Forming Using the Dynamite Finite Element Method, In: *PPS 2003, The Polymer Processing Society Europe/Africa Regional Meeting, CD-ROM Proceedings*, 14–17 September, Athens, Greece.
14. Feng, W. W. (1992). Viscoelastic Behavior of Elastomeric Membranes, *Journal of Applide Mechanics*, **59**: S29–S34.
15. Kyriacou, S. K., Schwab, C. and Humphrey, J. D. (1996). Finite Element Analysis of Nonlinear Orthotropic Membranes , *Comput. Mech.*, **18**(1): 269–278.
16. Lapidus, L. and Pinder, G. F. (1982). *Numerical Solution of Partial Differential Equations in Science and Engineering*, ISBN: 0-471-35944-0, John Wiley & Sons Inc.
17. Laroche, D. and Erchiqui, F. (2000). Experimental and Theoretical Study of the Thermoformability of Industrial Polymers, *Journal of Reinforced Plastics and Composites*, **19**(3): 231–239.
18. Liu, I. S. (1982). On Representation of Anisotropic Invariants, *International Journal Engng, Sci.*, **20**: 1099–1109.
19. Lodge, A. S. (1964). *Elastic Liquids*, Academic Press, London.
20. Ogden, R. W. (1972). Large Elastic Deformation Isotropic Elasticity – On the Correlation of Theory and Experiment for Incompressible Rubberlike Solids., *Proc. R. Soc. Lond.*, **A326**: 565–584.
21. Rivlin, R. S. (1948). Large Elastic Deformation of Isotropic Materials – Iiv. Further Developments of the General Theory, *Phil. Trans. R. Soc.*, **A241**: 379–397.
22. Shrivastava, S. and Tang, J. (1993). Large Deformation Finite Element Analysis of Non-linear Viscoelastic Membranes with Reference to Thermoforming, *J. Strain Analysis*, **28**: 31–51.
23. Tanner, R. I. (1988). From A to BKZ in Constitutive Relations, *The Society of Rheologiy*, **32**: 673–702
24. Verron, E., Marckmann, G. and Peseux, B. (2001). Dynamic Inflation of Non-linear Elastic and Viscoelastic Rubberlike Membranes, *Int. Journal for Num. Methods in Engineering*, **50**(5): 1233–1251.
25. Weiss, J. A., Maker, B. N. and Govindjee, S. (1996). Finite Element Implementation of Incompressible, Transversely Isotropic Hyperelasticity, *Computer Methods in Applied Mechanics and Engineering*, **135**: 107–128.
26. Weiss, J. A. and Puso, M. A. (1998). Finite Element Implementation of Anisotropic Quasi-linear Viscoelasticty using a Discrete Spectrum Approximation, *Journal of Biomech. Engng*, **120**: 62–70.